Urine production rate is critical in a model for catheter-associated urinary tract infection

Freya Bull,[1] Sharareh Tavaddod,[1] Nick Bommer,[2] Meghan Perry,[3] Chris A. Brackley,[1] and Rosalind J. Allen[1,4,*]

[1] *School of Physics and Astronomy, University of Edinburgh, Peter Guthrie Tait Road, Edinburgh EH9 3FD, UK*

[2] *Veterinary Specialists Scotland, Livingston, UK*

[3] *Regional Infectious Diseases Unit, Western General Hospital, Edinburgh*

[4] *Theoretical Microbial Ecology Group, Institute of Microbiology, Faculty of Biological Sciences, Friedrich Schiller University Jena, Buchaer Strasse 6, 07745 Jena, Germany*

Abstract

Catheter associated urinary tract infections (CAUTI) are of great societal and economic importance, yet there is limited understanding of how CAUTI develops. We present a mathematical model for bacterial colonisation of a urinary catheter, that integrates population dynamics and fluid dynamics. Our model describes bacteria growing and colonising the extraluminal surface, spreading into the bladder and growing there before being swept through the catheter lumen. In this scheme, the rate of urine production by the kidneys emerges as a critical parameter, governing a transition between regimes of high and low bacterial density in the bladder. This transition occurs at urine production rates close to that of the average human, highlighting the therapeutic importance of increasing fluid intake. Our model reveals how the time to detection of bacteriuria (bacteria in the urine) and the time to formation of a biofilm that may subsequently block the catheter depend on characteristics of the patient, the catheter, and the infecting bacterial strain. Additionally, patterns of bacterial density on infected catheters may provide clues about the source of infection.

*To whom correspondence should be addressed: `rosalind.allen@uni-jena.de`

Urinary catheters – thin tubes which are inserted into the urethra to drain the bladder – are commonly used in a wide range of patients with urological issues, in intensive care units and long term care facilities [1, 2]. Patients with catheters are prone to develop bacterial catheter-associated urinary tract infections (CAUTI) at rates estimated at up to 0.3–0.7% per catheter day [3, 4], with potential complications including catheter blockage, bladder damage, and kidney infections. CAUTI are extremely prevalent – accounting, for example, for up to 40% of hospital acquired infections [2–8] – with vast financial and societal costs [9]. Despite the importance of this topic, there is limited understanding of the role of different factors in CAUTI development [3, 4, 10–13], why some patients are plagued by recurrent CAUTI while others are hardly troubled [14], and why some infections develop far more rapidly than others [15]. Moreover, to date there have been no predictive mathematical models for bacterial colonisation of a urinary catheter. Better understanding of this process could lead to more effective strategies to prevent or mitigate CAUTI [16].

In this study we present a quantitative model for the dynamics of bacterial colonisation of a urinary catheter, which identifies parameters that are critical for clinical outcome. We do not attempt to model CAUTI directly, as by definition this entails symptoms (i.e. a physiological response from the patient) [17]. Our study focuses on the indwelling Foley catheter, in which the catheter tip sits inside the bladder, held in place by a balloon, while the catheter tubing passes through the urethra, terminating at an external drainage bag. We model the population dynamics of infecting bacteria as they migrate up the catheter, proliferate in the residual sump of urine that remains in the bladder during the period of catheterisation [9, 18–20], and travel out of the bladder in the urine flow through the catheter lumen, where they can attach to the inner lumen surface [4] and trigger biofilm formation that can block the catheter [3].

Combining these processes into a unified model allows us to predict the time course of CAUTI establishment and to identify the key parameters controlling clinical observables such as bacterial density in the bladder, the time before bacteriuria (bacteria in the urine) is detected, and the time to formation of a luminal biofilm. These parameters include the rate of urine production by the kidneys, the volume of residual urine in the bladder, and the length of the urethra. We find that the rate of urine production governs a transition between a high-density bladder state (bacteriuria) and a diluted, "washed out" state with low bacterial density. We also show how different spatial patterns of bacterial biofilm growth are expected on the catheter depending on the initial conditions, suggesting that it might be possible to infer the source of infection from these patterns.

Mathematical model for CAUTI establishment

Our model consists of four parts: the extraluminal surface of the catheter, the bladder, the urine flow within the catheter, and the intraluminal surface of the catheter (Fig. 1). These are coupled such that an infection may start anywhere within the system, allowing for all the major infection pathways (extraluminal, intraluminal, contamination on insertion), as well as for an infection originating in the bladder (e.g. after a catheter is replaced). The catheter is treated as a rigid open cylindrical tube, with rotational symmetry. The bladder is assumed to be well-mixed with the rate of urine production and the volume of residual urine assumed to be constant within each period of catheterisation. We model a monospecies infection and base our parameters on *E. coli*, which is present in 40–70% of CAUTI [3]. Numerical simulation of the model leads to predictions for the dynamics of the bacterial infection on the catheter and in the bladder. Full details of the model and its implementation, as well as background information, are given in Materials & Methods and the appendices.

Extraluminal surface

Bacteria proliferate and spread on the outside surface of the catheter. This is modelled by a 1-dimensional Fisher-Kolmogorov-Petrovsky-Piskunov (FKPP) equation [21]. If the infection initiates at the base of the catheter, it will spread up the catheter in a wave-like manner (Fig. 2a).

Bladder

Bacteria proliferate in the residual sump of urine that remains in the bladder during catheterisation [9, 19, 20], and then are removed from the bladder by urine flow. To model this we combine a logistic growth model [21] with a constant dilution rate that depends on the rate of urine production by the kidneys (Fig. 2b).

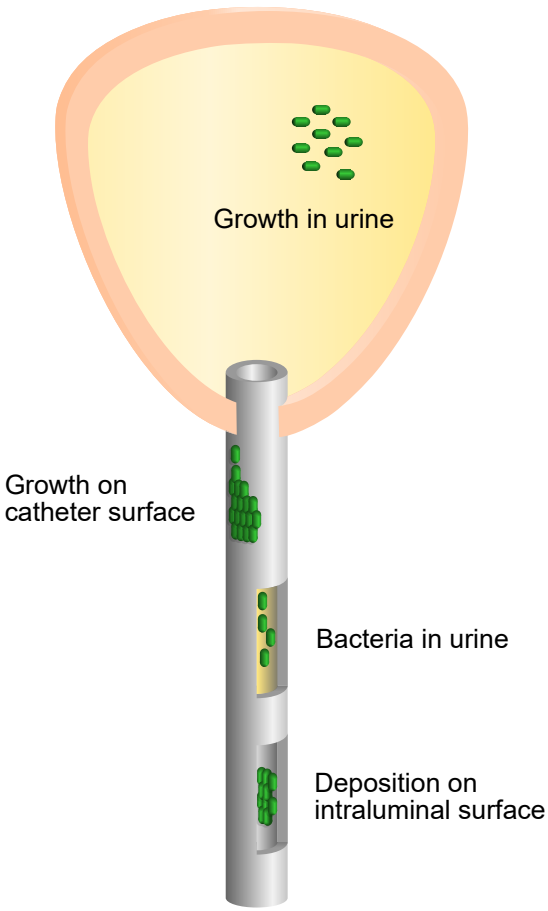

Figure 1: Sketch of the system being modelled. Bacteria grow and spread as a wave on the outside. They then grow in the residual urine within the bladder, before being transported downwards by the flow within the catheter. Some bacteria attach to the inside of the catheter, where they grow and spread just as on the outside.

Intraluminal flow

Urine leaving the bladder flows through the catheter lumen, transporting bacteria downwards. Some of these bacteria become stuck to the catheter surface, where they can form a biofilm. The bacterial density within the catheter is modelled with a convection-diffusion equation (Fig. 2c), assuming a Poiseuille flow profile for the urine (Reynold's number ≈ 6). Attachment of bacteria to the intraluminal surface is incorporated as an absorbing boundary condition.

Intraluminal surface

Bacteria that have been deposited on the intraluminal surface proliferate and spread. This is modelled by a FKPP equation with an additional source term due to the deposition of bacteria from the urine flow.

Connecting the model parts

The bladder and extraluminal surface are connected by detachment and attachment of bacteria to the top of the catheter, the extraluminal and intraluminal surfaces are connected by bacterial migration across the top of the catheter, the bladder and intraluminal flow are connected by urine flow out of the bladder and the intraluminal flow and intraluminal surface are connected by bacterial deposition on the surface. In each case, the number of bacteria is

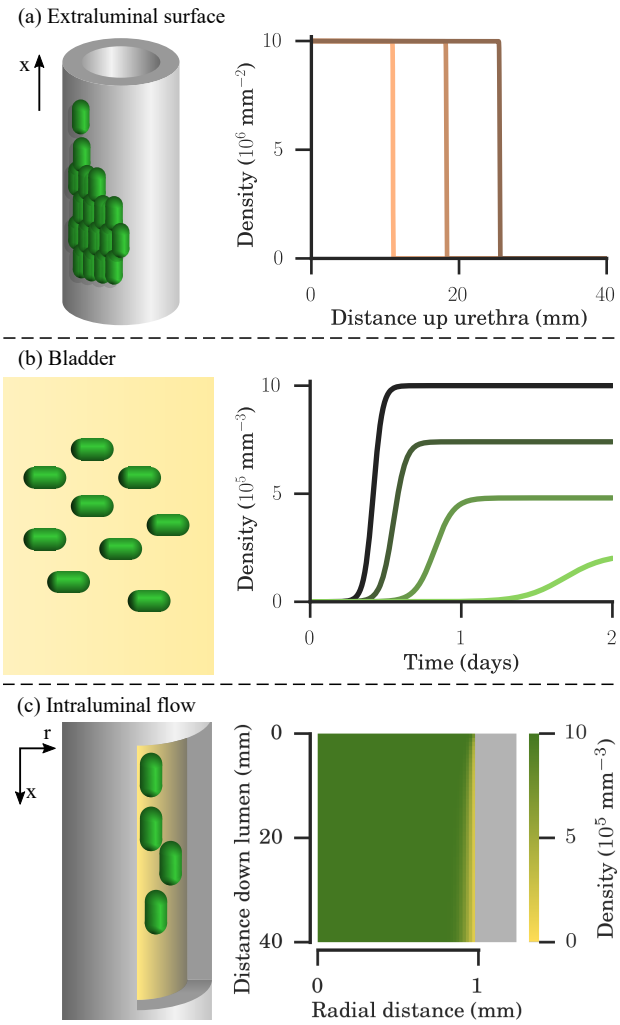

Figure 2: Illustration of the model components. (a) Left: bacteria grow and spread as a wave on the extraluminal surface. Right: behaviour of Eq. 1 (Materials & Methods) subject to open boundaries and an initial inoculation of 100 mm^{-2} at $x = 0$, with all parameters as given in Table I. Each curve is a snapshot of the density profile along the catheter at 30 (▬), 60 (▬) and 90 (▬) days respectively. (b) Left: bacteria grow in residual urine within the bladder. Right: behaviour of Eq. 2, with an initial inoculation of 1 mm^{-3}, subject to different dilution rates k_D. Each curve is a numerical solution for the bacterial density, with dilution rates of 0 (▬), 1 (▬), 2 (▬), and 3 (▬) $\times 10^{-4}$s^{-1} respectively. (c) Left: urine transports bacteria downwards through the catheter. Right: numerically solving Eq. 3 gives the distribution of bacteria within the catheter. At $x = 0$ there is a uniform bacterial density in the urine flowing from the bladder of 10^6 mm^{-3}. The urine becomes depleted of bacteria close to the surface due to bacterial deposition.

conserved (see Materials & Methods).

Materials & Methods

Extraluminal surface

Bacterial growth and spreading on the outside surface of the catheter is modelled in 1-dimension, the distance x up the catheter (Fig. 2a), using an FKPP equation [21]:

$$\frac{\partial n}{\partial t} = D_S \frac{\partial^2 n}{\partial x^2} + n r_S \left(1 - \frac{n}{\kappa_S}\right). \tag{1}$$

Here, $n(x,t)$ is the bacterial surface density at point x at time t, D_S the diffusivity of the bacteria on the catheter surface, r_S the bacterial growth rate on the catheter surface, and κ_S the bacterial carrying capacity of the catheter surface (see Table I).

Bladder

Assuming the residual urine in the catheterised bladder [9, 19, 20] to be well-mixed and of constant volume, we model bacterial dynamics with a logistic growth equation, supplemented by a dilution term [21]:

$$\frac{d\rho}{dt} = r_B\rho\left(1 - \frac{\rho}{\kappa_B}\right) - k_D\rho. \tag{2}$$

Here, $\rho(t)$ is the bacterial volume density at time t, r_B is the (maximum) growth rate of the bacteria in urine, and κ_B is the carrying capacity of urine. The dilution rate is given by $k_D = \frac{\lambda}{V}$, where λ is the rate of urine production by the kidneys, and V is the volume of residual urine in the bladder (see Table I and appendices) .

Intraluminal flow

Transport of bacteria in the urine that flows through the catheter lumen is modelled with a 2-dimensional convection-diffusion equation [22, 23], in the radial distance r and the longitudinal distance down the catheter x (geometry illustrated in Fig. 2c):

$$\begin{aligned} \frac{\partial\sigma}{\partial t} &= D_B\left(\frac{\partial^2\sigma}{\partial r^2} + \frac{1}{r}\frac{\partial\sigma}{\partial r}\right) - u(r)\frac{\partial\sigma}{\partial x} \\ u(r) &= \frac{2\lambda}{\pi R^4}\left(R^2 - r^2\right). \end{aligned} \tag{3}$$

Here $\sigma(r,x,t)$ is the bacterial volume density in the urine, D_B is the diffusivity of bacteria within urine, and $u(r)$ is the flow profile of the urine, with R being the internal radius of the catheter, and λ the rate of urine production. A Poiseuille flow profile is expected, since the Reynold's number is ≈ 6 (see the Supplemental material for further justification).

Intraluminal surface

Bacterial growth and spreading on the intraluminal surface is modelled with a 1-dimensional FKPP equation, supplemented with a source term $j(x)$ accounting for deposition of bacteria from the urine (see Eq. 11 below):

$$\frac{\partial m}{\partial t} = D_S\frac{\partial^2 m}{\partial x^2} + r_S m\left(1 - \frac{m}{\kappa_S}\right) + j(x). \tag{4}$$

Here, $m(x,t)$ is the bacterial surface density; D_S, r_S, and κ_S are the diffusivity, growth rate, and carrying capacity (as above).

Connecting the extraluminal surface and bladder

Bacterial transfer from the top of the extraluminal surface to the bladder is incorporated by adding the following term to the right hand side of Eq. 2:

$$\frac{k_d S_c n(L,t) - k_a V_c \rho(t)}{V}, \tag{5}$$

where V is the volume of residual urine in the bladder, $n(L,t)$ is the bacterial surface density at the top of the catheter, S_c is the area of catheter surface in contact with the bladder, V_c is the volume of urine surrounding the catheter into which bacteria can transfer, and k_d and k_a are respectively the rates at which bacteria detach from and attach to the catheter surface. Bacterial transfer in the other direction, from the bladder to the extraluminal surface,

is incorporated by a corresponding surface density flux at the top of the catheter, which is added to the right hand side of Eq. 1:

$$\frac{k_a V_c \rho(t) - k_d S_c n(L,t)}{S_c}. \tag{6}$$

These coupling terms are derived in the appendices.

Connecting the extraluminal and intraluminal surfaces

Since we do not model the catheter eyelets, we assume that bacteria can spread freely across the top of the catheter between the extraluminal and intraluminal surfaces. This is represented by a continuity condition on the bacterial density, connecting Eqs. 1 and 4:

$$n(x{=}L,t) = m(x{=}0,t), \tag{7}$$

where L is the length of the catheter.

Connecting the bladder and intraluminal flow

To ensure continuity of bacterial density in the urine leaving the bladder and entering the lumen, we impose the following coupling between Eqs. 2 and 3:

$$\sigma(r, x{=}0, t) = \rho(t). \tag{8}$$

Connecting the intraluminal flow and intraluminal surface

Deposition of bacteria from the urine onto the intraluminal surface is incorporated via an absorbing boundary condition for Eq. 3, i.e. the catheter wall is assumed to be a perfect sink. Deposition onto the surface depletes the urine of bacteria close to the surface (Fig. 2c). The flux of deposited bacteria appears as the source term $j(x)$ for the intraluminal surface in Eq. 4. To calculate this flux, we compute the rate at which bacteria hit the boundary $r = R$ for the longitudinal distance x down the catheter:

$$j(x) \cdot 2\pi R = \int_0^{2\pi} \int_R^{\infty} \frac{\partial \sigma(r,x,t)}{\partial t}\ r\ \mathrm{d}r\mathrm{d}\psi. \tag{9}$$

Applying Eq. 3 gives

$$\begin{aligned} j(x) &= \frac{1}{R} \int_R^{\infty} D_B \left(\frac{\partial^2 \sigma}{\partial r^2} + \frac{1}{r}\frac{\partial \sigma}{\partial r} \right)\ r\ \mathrm{d}r \\ &= -D_B \left. \frac{\partial \sigma}{\partial r} \right|_{r=R}. \end{aligned} \tag{10}$$

This flux can be obtained either by numerical solution of Eq. 3, or by an analytic approximation [24], which gives

$$j(x) = 0.5835 D_B \rho \sqrt[3]{\frac{\lambda}{R^3 D_B}} \frac{1}{\sqrt[3]{x}}. \tag{11}$$

Details of the analytical approximation leading to Eq. 11 can be found in the appendices.

Model implementation

The model was simulated numerically using a forward-time centred-space (FTCS) method for the extraluminal and intraluminal surface and a forward Euler method for the bladder. An approximate analytical solution for the bacterial flux onto the intraluminal surface was used to reduce the computational requirements (see appendices).

Parameter		Default value in simulations	Justification and expected range
Urethral length	L	40 mm	Women: 40 mm. Men: 160 mm [9]
Residual urine volume	V	50 ml = 5×10^4 mm^3	$10-100$ ml [9], may be up to 500 ml in immobile patients [20]
Urine production rate	λ	1 ml min^{-1} = 16.7 mm^{3}s^{-1}	1 ml min^{-1} [9]
Dilution rate	k_D	1.2 hr^{-1} = 3.33×10^{-4} s^{-1}	$k_D = \lambda/V$
Catheter internal radius	R	1 mm	Outer diameter: 4-5 mm [9], wall thickness is manufacturer dependent
Bacterial surface diffusivity	D_S	10^{-2} μm^{2}s^{-1} = 10^{-8} mm^{2}s^{-1}	10^{-2} μm^2 s^{-1} for *P. aeruginosa* [25]
Bacterial bulk diffusivity	D_B	10^2 μm^{2}s^{-1} = 10^{-4} mm^{2}s^{-1}	100 μm^2 s^{-1} for *E. coli* [26]
Catheter surface bacterial growth rate	r_S	0.69 hr^{-1} = 1.93×10^{-4} s^{-1}	Doubling time of *E. coli* on poor media is $\sim$ 1 hr [27]
Bacterial growth rate in bladder	r_B	1.39 hr^{-1} = 3.85×10^{-4} s^{-1}	Doubling time of *E. coli* in UTIs is 30-35 mins [28]
Catheter surface carrying capacity	κ_S	10^9 cm^{-2} = 10^7 mm^{-2}	Biofilms of 5×10^9 cm^{-2} have been found on catheters [29]
Bladder carrying capacity	κ_B	10^9 ml^{-1} = 10^6 mm^{-3}	*E. coli* in mice [28]: 10^8 CFU g^{-1} and in LB [30]: 10^9 cells mL^{-1}
Bacterial detachment rate	k_d	1.93×10^{-4} s^{-1}	Assume that all new growth detaches: $k_d = r_S$
Bacterial attachment rate	k_a	1.26×10^{-6} s^{-1}	Smoluchowski diffusion rate limited constant [31]: $4\pi D_B\cdot 1$ μm

Table I: Model parameters. The values used in the model are listed together with the expected range of values for each parameter.

Parameters

Table I lists the parameters used in our model, their values and their expected range in a clinical setting.

Results

A. Urine production rate drives a transition in bacterial density

The rate of urine production by the kidneys is correlated with the fluid intake of the patient. This is a key parameter in our model, since it controls the rate at which bacteria are removed from the bladder by dilution (denoted by k_D; see Eq. 2 in Materials & Methods) and the rate of urine flow through the catheter lumen (denoted by λ; see Eq. 3 in Materials & Methods), which in turn determines the rate of bacterial deposition on the intraluminal surface. Previous (uncatheterised) micturition models have suggested a critical dependence between the urine production rate and the bacterial growth rate in the bladder [18]. Therefore we investigated how the behaviour of our model depends on the rate of urine production.

We observed a critical transition upon varying the urine production rate (Fig. 3). At low production rates, the bacterial population density within the bladder is high, since bacteria can grow fast enough to overcome dilution. At high urine production rates, the population density in the bladder falls dramatically, as the dilution rate exceeds the maximal rate at which the bacteria can grow. This transition is continuous in the first order, with a near-linear dependence of the steady state bacterial population density on the urine production rate (Fig. 3 lower inset); however the time taken to attain this steady state diverges at the critical urine production rate (Fig. 3 upper inset). A typical value for urine production rate in humans is 16.7 mm^{3}s^{-1} (i.e. 1 mL min^{-1}; dashed line in Fig. 3) [9]. This value lies very close to the critical threshold predicted by our model (Fig. 3), suggesting that individual patients might show dramatically different levels of bacteriuria (bacteria in the urine) depending on their fluid intake.

This transition is essentially a washout phenomenon, as observed in continuous culture, where bacteria grow in continuously diluted medium and it is well known that a bacterial population can only be sustained for dilution rates less than the bacterial growth rate [32, 33]; as well as in a previous study of an uncatheterised micturation model [18]. Indeed, when plotted on a linear scale (Fig. 3 lower inset), the transition in the catheter model appears indistinguishable from washout, with the bacterial density approaching zero as the urine production rate approaches

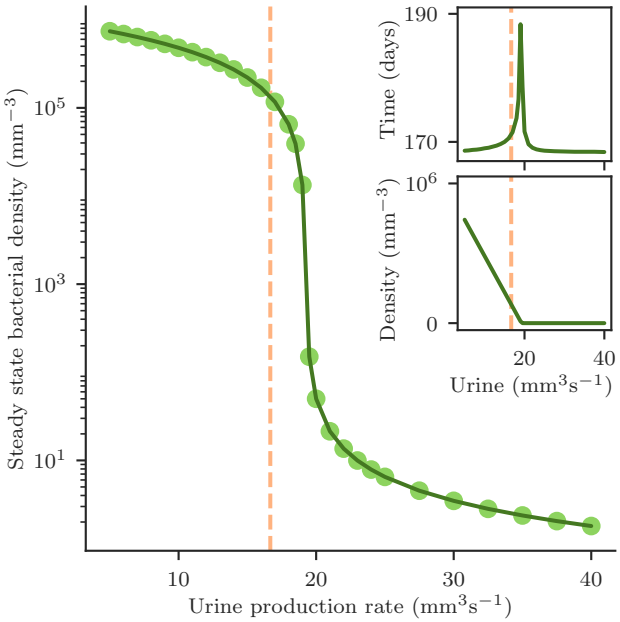

Figure 3: Transition driven by urine production rate. As the rate of dilution of the bladder increases beyond the bacterial growth rate, there is a transition from a high density bladder state to a 'washed out' state. Each point represents a bacterial density obtained from a numerical simulation. Lower inset shows the same data on a linear scale. Upper inset shows the time taken to attain the maximum density, with a sharp peak at the transition. Also plotted (▬) is the typical urine flow rate in a patient, 1 mL min^{-1} [9].

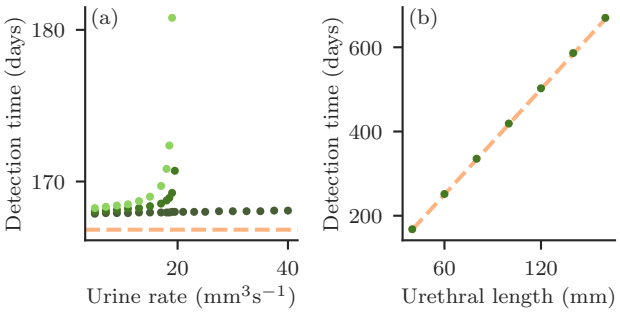

Figure 4: Time to detection of bacteriuria, for tests of varying sensitivities. We plot the times until the bacterial volume density in the urine exceed 10^4 (●), 10^2 (●), and 1 (●) mm^{-3} respectively. Also plotted (▬) is the time for the Fisher wave to spread across the extraluminal surface, $L/2\sqrt{r_S D_S}$. (a) Varying the urine production rate. (b) Varying the urethral length. Note that in this case there is no significant difference between different testing sensitivities, as the urethral length dominates the timescale. All parameters are as given in Table I.

the bacterial growth rate. However, in the logarithmic plot (Fig. 3 main), we observe a "tail" that is due entirely to re-population of the bladder from bacteria that have adhered to the catheter surfaces. Without this bacterial migration from the catheter surface to the residual urine sump, the bacterial density in the urine would fall to zero at the transition (see appendices). The presence of the catheter "smooths" the transition, such that even at high urine production rates some bacteria are still present in the urine. Hence, the presence of the catheter allows the infecting bacterial population to persist even if the urine production rate is high enough to wash it out of the bladder. Indeed, catheter-associated biofilms are known to act as a bacterial reservoir, leading to persistent re-infection of the bladder [34].

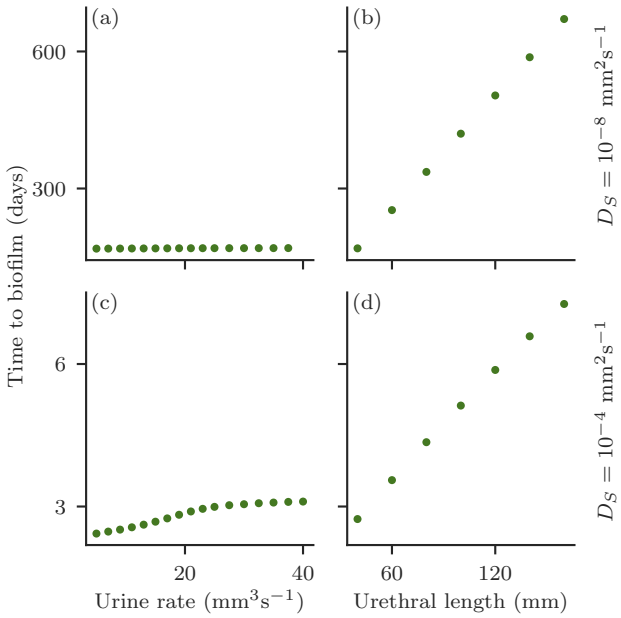

Figure 5: The interplay of physical parameters and bacterial characteristics on the timescale of biofilm formation. We plot the time taken for the maximum bacterial surface density on the catheter lumen to exceed 10^7 mm^{-2}. Left, (a) and (c), varying the urine production rate. Right, (b) and (d), varying the urethral length. Upper, (a) and (b), have a bacterial surface diffusivity of 10^{-8} mm^{2}s^{-1}. Lower, (c) and (d), have a bacterial surface diffusivity of 10^{-4} mm^{2}s^{-1}. All other parameters are as given in Table I.

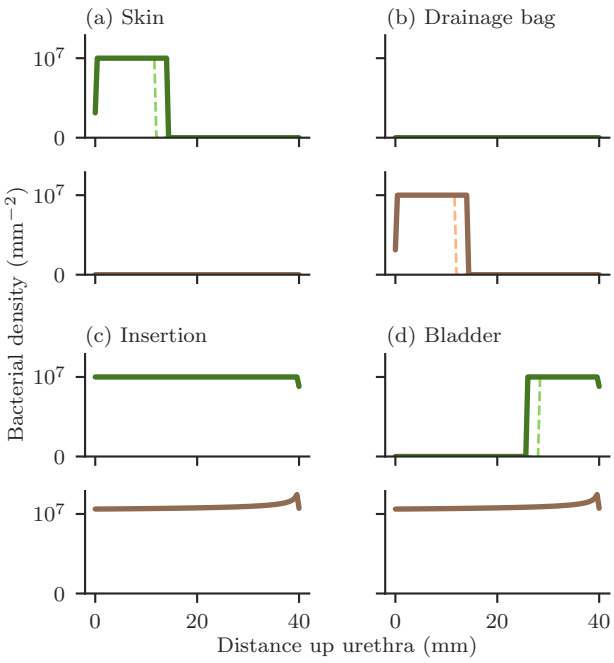

Figure 6: Bacterial density patterns for four different infection scenarios. We plot the bacterial surface density for: the extraluminal surface, after 50 days (- - -) and 60 days (▬); and the intraluminal surface after 50 days (- - -) and 60 days (▬). Here a distance 0 mm up the urethra is the skin or drainage bag boundary, and 40 mm the bladder boundary, all parameters are as given in Table I. (a) The skin acts as a reservoir from which infection can spread. (b) The drainage bag becomes contaminated, and bacteria ascend the catheter lumen. (c) The catheter is inoculated uniformly at time of insertion. (d) Bacteria are already present in the bladder prior to insertion.

B. Time to detection of bacteriuria is controlled by movement of bacteria up the catheter

The appearance of bacteria in the urine, bacteriuria, is an almost inevitable consequence of long-duration catheterisation [35], with an occurrence rate of 3–7% per catheter day [10] (bacteriuria occurs more frequently than CAUTI, which has an occurrence rate of 0.3–0.7% per catheter day [3, 4]). In the absence of other symptoms, asymptomatic bacteriuria does not imply that the patient has CAUTI, but can often be erroneously treated as CAUTI [17]. By tracking the density of bacteria in the outflowing urine, our model can predict how long after catheter insertion bacteriuria will be detected, assuming a certain detection sensitivity. Here we assume that infection is initiated by bacteria on the outside of the catheter, where the urethra meets the skin (see Materials & Methods).

For high-sensitivity tests (detection at cell counts of 1 mm^{-3}, i.e. 10^3 mL^{-1}), our model predicts that bacteriuria will eventually be detected, no matter how high the urine production rate (Fig. 4a). This is because, even in the "washout" regime (Fig. 3) the presence of the catheter ensures that there are some bacteria in the urine. The time to detection of bacteriuria is almost independent of the urine production rate, since the detection time is dominated by the time for bacteria to migrate up the extraluminal surface. This implies that early removal of the catheter can prevent occurrence of bacteriuria, since bacteria do not have time to reach the bladder. Indeed, the duration of catheterisation is known to be the single biggest risk factor for developing CAUTI [4, 10, 13]. In contrast, low sensitivity tests (requiring cell counts $> 10^2$ mm^{-3}, i.e. 10^5 mL^{-1}) will never detect bacteriuria in the high urine production rate regime (Fig. 4a), even though some bacteria are present in the urine (Fig. 3). This is because the steady-state bacterial density is below the detection threshold. Strikingly, some clinical guidelines [4] distinguish different thresholds for diagnosis of CAUTI and bacteriuria. For CAUTI, these guidelines require bacterial counts $> 10^3$ CFU mL^{-1} (equivalent to our high sensitivity threshold; CFU = colony forming units, a proxy for cell count) as well as symptoms, while bacteriuria requires a higher bacterial count $> 10^5$ CFU mL^{-1} (equivalent to our low sensitivity values).

The time to detection of bacteriuria depends linearly on the length of the catheter, which corresponds to the length of the urethra (Fig. 4b). This is because the timescale of bacterial migration up the extraluminal surface is set by the speed of the FKPP wave (Eq. 1). The main factor determining urethral length in humans is gender, with a typical length for a woman being 40 mm, and for a man 160 mm [9]. This result is therefore consistent with the fact that gender is a well-established risk factor for CAUTI [4, 13].

C. Time to formation of a biofilm depends on characteristics of the patient, catheter and infecting bacteria

Catheter blockage is a frequent and serious complication of CAUTI. Most commonly, blockage is caused when biofilms of *Proteus mirabilis* form on the catheter surface and increase the urine pH, causing crystals to precipitate [36, 37]. However, non-crystalline biofilms of other uropathogens such as *E. coli* can also disrupt urine flow [19, 29]. Our model cannot directly predict catheter blockage, since we do not model biofilm-associated changes in urine flow. However, as a proxy, we predict the time until the value of the surface density of bacteria at any point on the intraluminal surface reaches a threshold of 10^7 bacteria per mm^2 (corresponding roughly to a monolayer), which we term "time to biofilm".

In our model, the time to biofilm formation depends on the characteristics of the human patient, of the catheter and of the infecting bacteria. Assuming that the infection starts on the external base of the catheter, bacteria must migrate up the catheter before they can populate the intraluminal surface. Bacterial migration up the catheter depends on urethral length and on bacterial surface motility (Eq. 1); altering either of these parameters has a drastic effect on the time to biofilm formation (compare Figs. 5b and 5d with bacterial surface diffusion coefficients of 10^{-8} mm^2s^{-1} and 10^{-4} mm^2s^{-1}).

The urethral length determines the timescale of migration on the extraluminal surface, while the urine production rate determines the timescale of bacterial growth (bacteriuria) in the bladder. The relative contributions of these two timescales to the overall infection timescale are determined by the bacterial characteristics (Fig. 5; see appendices for the dimensionless number). When the bacterial motility is low, the effect of varying the urine rate is negligible (Fig. 5a) compared to varying the urethral length (Fig. 5b) – this is the surface dominated regime. But when the bacterial surface motility is higher, varying the urine rate has a significant effect (Fig. 5c), on a comparable timescale to varying the urethral length (Fig. 5d) – this is a mixed regime, with both bladder and surface affecting the overall timescale. Notably, the bacterial surface motility is the model parameter which is least well-defined in the literature. In particular, surface motility is highly dependent on the surface "wetness" (Table I).

D. Different sources of infection produce different patterns of biofilm

Most CAUTI are thought to originate extraluminally, originating, for example, from the gastrointestinal tract via the skin of the meatus and perineum [36, 38, 39]. However, CAUTI can also arise when bacteria contaminate the drainage bag or port and ascend the intraluminal surface of the catheter [38]. A third pathway is contamination during catheter insertion, which is thought to account for around 5% of CAUTI [3]. Infection sources within the bladder are also possible, either because of a urinary tract infection prior to catheterisation or because of persistent intracellular bacterial communities in the epithelial cells that line the bladder [36, 40]. In our model, different sources of infection lead to different patterns of bacterial density on the extraluminal and intraluminal surfaces of the catheter as the infection develops (Fig. 6) – even though the model always predicts eventual complete coverage of both surfaces by bacteria.

If the infection originates on the outside, at the catheter base (i.e. from the skin), a wave of bacteria spreads up the extraluminal surface. At early times, therefore, the model predicts high bacteria coverage on the lower part of the extraluminal surface only, while the upper extraluminal surface and intraluminal surface are still uncolonised (Fig. 6a). If the infection instead originates at the base of the intraluminal surface (e.g. from the drainage bag), the bacterial wave instead spreads up the inner surface, so that at early times, bacterial coverage is high only on the lower intraluminal surface (Fig. 6b). Note that within these results we assume the intraluminal surface to be the same length as the urethra; in practice there is an additional length beyond the urethra, connecting to the drainage bag, and we would expect infections ascending from the drainage bag to have longer establishment times than infections from another scenario. For an infection that originates in the bladder, the entire intraluminal surface rapidly becomes colonised and a bacterial wave also propagates down the extraluminal surface from the top (Fig. 6c). Finally, if the infection originates on catheter insertion, such that bacteria become spread all over the extraluminal surface, the model predicts very rapid bacterial growth across the entire surface (Fig. 6d).

Therefore this model predicts that while catheters that have been in place for long times will show similar patterns of bacterial colonisation, catheters that are examined sooner, before any infection is fully established, may have qualitatively different distributions that reflect the source of their infection. Measuring patterns of bacterial density on clinical catheter samples might provide a way to test these predictions.

Discussion

Despite the high prevalence of CAUTI, and its societal and economic costs, much remains to be understood about how bacteria colonise urinary catheters. In this work, we formulated a mathematical model that integrates bacterial population dynamics on the catheter surfaces and in the bladder with urine flow. Bacteria migrate on the external catheter surface, populate the bladder, and flow in the urine through the catheter lumen where they can attach to and colonise the surface. The model is consistent with clinical observations that nearly all long-term catheterisations result in bacteriuria [3, 16], and that catheterisation duration and gender are important risk factors for CAUTI [35, 41].

We studied in detail how the characteristics of the patient, the catheter and the infecting bacteria influence bacterial density in the bladder, the time to detection of bacteriuria, the time to formation of a biofilm (a proxy for blockage), and the spatial patterns of bacteria on the catheter. The model points to urine production rate as a key parameter controlling a transition between regimes of high and low bacterial density in the bladder. Typical human urine production rates lie close to the predicted threshold (here determined by the growth rate of uropathogenic *E. coli*), suggesting that individual patients might show dramatically different levels of bacteriuria depending on their fluid intake. Drinking more water is known to be protective against urinary tract infections [18, 42–44]. For CAUTI, previous work suggests that dilution of the urine prevents its alkalisation, and hence crystallisation, by *P. mirabilis* [45]. Our work suggests that increased fluid intake can also delay catheter blockage by decreasing the density of bacteria in the urine and hence slowing down colonisation of the lumen.

The time taken by bacteria to migrate up the catheter is also an important factor, since it dominates the time to detection of bacteriuria and influences strongly the time to formation of a biofilm. Since migration time depends linearly on urethral length, our model predicts that women will develop bacteriuria faster than men. Gender is already a known risk factor for all urinary tract infections, with many reports of greater prevalence in women than in men [41, 46, 47]. Our model suggests that catheters will always get colonised by bacteria eventually, but that this happens faster in women than in men. Catheters are typically removed after a fixed time. If the timescale of catheterisation is short (as in many hospital settings), our model would indeed predict a higher incidence of observed bacteriuria in women than in men.

CAUTI is defined as a symptomatic infection that should be treated by catheter removal and possibly antibiotics; in contrast, asymptomatic bacteriuria may not need to be treated [3, 4]. Our model does not describe the human response to bacterial infection, so cannot predict the presence or absence of symptoms such as pain or fever. However, it does

make a clear distinction between bacteriuria and bacterial colonisation of the catheter lumen (i.e. biofilm formation). In the model, bacteriuria happens earlier than biofilm formation – suggesting that detection of bacteriuria does not necessarily imply a colonised catheter. Interestingly, the model also predicts that a catheter could block without bacteriuria being detected at all. This happens in the regime of high urine flow, where the bacterial density in the urine is low but the lumen can still become colonised.

Inspecting the spatial patterns of biofilm on infected catheters could provide a way to test our model, as well as a pointer to the origin of an infection. Such measurements are not routinely performed, but intriguingly, a study of central venous catheters [48] observed that while biofilm formation was universal, the extent and location of biofilm formation depended on the duration of catheterization: short-term catheters had greater biofilm formation on the external surface while long-term catheters had more biofilm formation on the inner lumen. These observations are similar to our model predictions, suggesting that closer observation of the nature of the biofilm on infected urinary catheters could be highly informative.

Acknowledgments

This paper is dedicated to the memory of Professor Fiona Denison (1970-2022). The authors acknowledge valuable discussions with Aidan Brown, Craig Breheny, Fiona Denison, Voula Granitsiotis, Gail McConnell, Freya Oswald, Liam Rooney, Alice Street, Bartlomiej Waclaw, Ellen Young and the NHS Lothian Bladder and Bowel Nurse Team. This work was supported by EPSRC via the Scottish Doctoral Training Centre in Condensed Matter Physics (grant number EP/L015110/1), by the European Research Council under Consolidator Grant 682237 EVOSTRUC and by the Scottish Universities Life Science Alliance via an AMR Seed Award. RJA was also supported by the Excellence Cluster Balance of the Microverse (EXC 2051 - Project-ID 390713860) funded by the Deutsche Forschungsgemeinschaft (DFG). For the purpose of open access, the author has applied a Creative Commons Attribution (CC BY) licence to any Author Accepted Manuscript version arising from this submission.

Appendix A: Background

The Foley catheter

A urinary catheter is a tube that is used to drain urine from the bladder into a drainage bag. Catheterisation can be intermittent (*i.e.* the catheter is removed immediately after drainage), but here we focus on longer-term catheterisation, where the catheter is indwelling (*i.e.* the catheter remains in the bladder). An indwelling catheter is inserted into the bladder through the urethra, or through a hole in the abdomen (suprapubic catheter). This can occur in a hospital setting, commonly during and after surgery, or in a long-term care setting. Catheterisation is extremely common: over 90,000 people live with an indwelling catheter in the United Kingdom [49].

In this study, we focus on the indwelling Foley catheter. This type of catheter is a flexible tube that is inserted into the bladder via the urethra. The tube contains two lumens. Sterile water is injected into one of the lumens after insertion, to inflate a balloon just below the catheter tip. This balloon holds the catheter in place. The other lumen is used to drain urine. It has holes (eyelets) close to the catheter tip through which urine passes from the bladder, before flowing through the lumen into a drainage bag outside the body. Typical flow rates for urine passing through the catheter are 1 mL min^{-1} [9]. Catheter lengths range from 40 mm for women up to 160 mm, or greater, for men, with the balloon having a volume of 10 mL [9]. Modern catheters are typically made of latex or silicone, with external cross-sectional diameters of 4.0–5.3 mm (catheters are generally sized in French gauge, where 3 Fr = 1 mm; typical catheters are sized between 12 and 16 Fr) [9]. The Foley catheter remains close to its original 1930s design, although a closed drainage system (to reduce contamination from the drainage bag) was successfully introduced in the 1960s [29, 50].

Catheter-associated urinary tract infection (CAUTI)

Urinary catheters are, unfortunately, prone to bacterial infection. When such an infection is symptomatic, *i.e.* the patient has symptoms such as fever, pain or inflammation, it is known as a catheter associated urinary tract infections (CAUTI). CAUTI are a regular part of life for patients with long-term indwelling catheters, with some studies finding rates of symptomatic episodes as high as 1.1 per 100 catheterised patient-days [4]. CAUTI is also prevalent in hospital settings: in fact, CAUTI accounts for up to 40% of hospital acquired infections [2–8]. CAUTI incurs huge economic costs; for example, it is estimated to cost the United Kingdom £1.0 - £2.5 billion annually [9].

Despite the prevalence of CAUTI, there is still limited understanding of the importance of different factors in the development of infection [3, 4, 10–12]. Understanding these factors and their mechanisms may be a key step in reducing CAUTI's impact [16]. Perhaps then we might understand why some patients seem plagued by chronic infections, while others are hardly troubled, or why some infections seem to develop far more rapidly than other infections.

Risk factors for CAUTI include the duration of catheterisation [4, 10, 13]; gender, with prevalence of CAUTI significantly higher in female hospital patients than males [13, 51]; and dehydration [29, 52].

Bacterial pathogens causing CAUTI

The bacterial pathogens most commonly associated with CAUTI overlap substantially with those that cause urinary tract infections more generally. With or without a catheter, infections are primarily associated with uropathogenic *Escherichia coli* (UPEC), which is present in 75% of uncatheterised urinary tract infections [53], and in 40–70% of CAUTI [3]. Other bacteria commonly isolated from CAUTI include *Klebsiella* spp, *Enterococcus* spp, *Proteus mirabilis*, and *Pseudomonas aeruginosa*, and also yeast: *Candida* spp [3]. *P. mirabilis* has been the focus of attention in the context of CAUTI because of its tendency to form crystalline biofilms in the catheter lumen (see below, under "catheter blockage").

Bacteriuria

It is important to clarify the difference between CAUTI and asymptomatic bacteriuria. CAUTI is defined as a bacterial infection accompanied by symptoms (inflammation, fever, pain etc), whereas bacteriuria is the presence of bacteria within urine, which can occur without symptoms [4]. Bacteriuria is extremely prevalent, with occurring at a rate of 3-7% per catheter day [10], and hence almost all patients will develop bacteriuria if catheterised long enough [35]. Since CAUTI is distinguished from bacteriuria by the presence of symptoms – which our model cannot predict – when modelling bladder dynamics we are modelling the development of bacteriuria.

Bacterial colonisation of the catheter

A number of different factors contribute to the vulnerability of catheterised patients to CAUTI infections. The catheter surface provides a direct pathway for bacteria to enter the body, harbouring biofilms and providing access to the bladder. The catheter surface is particularly vulnerable to contamination at the meatus, potentially by gut bacteria. Moreover, the presence of a foreign object in the urethra and bladder can cause trauma to the tissues there, which in turn increases their susceptibility to infection. [3, 9, 19, 29]. The port connecting the catheter to the drainage bag also constitutes a potential point of vulnerability to infection. Although port is theoretically sterile, the need to regularly replace the drainage bag exposes it to possible contamination, particularly for patients in the community.

Catheterisation also changes the characteristics of the bladder as a site of infection. Even in the absence of a catheter, the bladder is known to retain a small volume of urine [18]; this is a rich growth medium [29] that can support high bacterial densities: up to 10^8 CFU g^{-1} (CFU = colony forming units; an experimental estimate for the number of viable cells in a sample), with doubling times of 30 mins for *E. coli* [28]. With indwelling catherisation, the volume of this residual sump is increased due to a combination of factors including the location of the catheter balloon and inlets, the cessation of tidal drainage in favour of continuous drainage, and hydrostatic pressure differentials, particularly as a result of kinks in the catheter tubing [20]. The prevention of tidal drainage also disrupts the self-cleaning nature of the bladder and urethra, preventing the regular flushing out of bacteria [2, 9]. It is likely that the epithelial cells that line the bladder walls also have a role to play in infections. Some patients experience recurrent urinary tract infections due to persistent intracellular bacterial communities in the epithelial cells [40]; the same mechanism could also cause recurrent CAUTI [36].

Thus, the catheter can act as a reservoir for bacteria to spread into the bladder, but so too can the residual urine within the bladder act as a reservoir from which the catheter can become infected.

It has been established that around two thirds of catheter-associated infections are extraluminal, i.e. originate from bacterial growth on the outside of the catheter [36]. Most of the remaining infections are attributed to bacteria infecting the drainage bag or port and then ascending the internal (intraluminal) surface of the catheter. Only around 5% of infections are due to contamination at the point of catheter insertion [3].

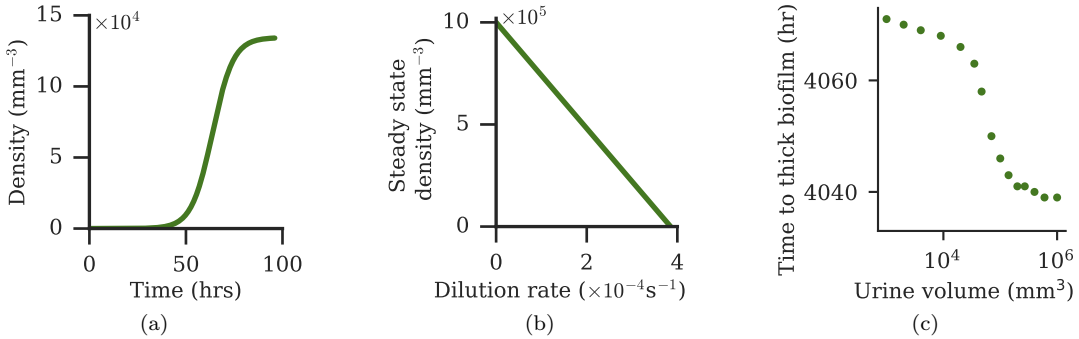

Figure 7: Importance of bladder parameters. (a) Behaviour of the bladder model (Eq. 2 of the main text) when uncoupled from the rest of the system: the dynamics of the bacterial density as the system approaches the steady state. Initial condition is $\rho(t{=}0) = 1$ mm^{-3}. (b) Dependence of the steady state solution of Eq. 2 on the dilution rate, k_D. The steady state bacterial density decreases linearly as the dilution rate increases. (c) The effect (in the full coupled model) of varying the residual urine sump volume on the time until the maximum bacterial surface density on the catheter lumen exceeds 10^7 mm^{-2}. All parameters except either the dilution rate or sump volume are as in table 1 of the main text.

Catheter blockage

CAUTI is not merely an unpleasant inconvenience for sufferers; it also brings risk of serious consequences, including kidney infections, bloodstream infections and tissue damage within the bladder [47]. A common consequence of CAUTI is blockage of the catheter, which will, at best, result in urine bypassing the catheter, and at worst can lead to the backflow of infected urine into the kidneys [53].

Catheter blockage is sometimes due to the formation of a thick biofilm by bacteria such as *Pseudomonas aeruginosa* [34], however more commonly the cause is crystalline biofilms formed by *Proteus mirabilis*[36, 45]. *P. mirabilis* hydrolyses urea, producing ammonia, which increases the alkalininty of the urine, leading to precipitation of crystals of struvite and apatite [36, 45].

Appendix B: Further model details

Bladder

We use a logistic equation to describe growth of bacteria in the bladder (Fig. 7a). Bacteria grow exponentially, and so the simplest possible model for bacterial growth in the bladder is exponential. This is the approach followed by Gordon and Riley [18] in their paper on micturition dynamics and urinary tract infections. However, an exponential growth model is unbounded, rapidly diverging toward infinite bacterial densities, rendering it unsuitable for modelling anything but early timescales. The simplest possible modification that can be made to exponential growth to enforce bounds is logistic growth.

Logistic growth is convenient, but has no physical or biological justification except that growth is finite and initially exponential. An alternate model is a chemostat: a device in which bacteria grow under conditions of continuous dilution, which closely resembles the situation of bacterial growth in a catheterised bladder. But chemostat theory can describe bacterial growth only on a single, simple limiting substrate, e.g. glucose as the sole carbon source. Urine is not a simple substrate, and so there is no existing chemostat model to describe bacterial growth in urine. It seems that for a minimal model, logistic growth may therefore be a reasonable approximation.

As discussed in the main text, the value of the dilution rate k_D (which is controlled by the urine production rate λ and the bladder volume V via $k_D = \lambda/V$) is critical to the behaviour of our model. The dilution rate governs both the steady state bacterial density in the bladder (Fig. 7b), and the timescale over which the steady state is attained (Main text Fig. 2b). This dependence of the model on the dilution rate is very similar to the behaviour of other (uncatheterised) micturition models, where there is a critical relationship between the urine dilution rate and the bacterial growth rate [18]. However in our model the presence of the catheter means that the bacterial density in the bladder does not go to zero in the high dilution rate "wash-out" state.

Since the urine production rate is incorporated into the bladder model through the dilution rate ($k_D = \lambda/V$), similar results to varying the urine production rate can be obtained by varying the residual urine sump volume in the bladder (Fig. 7c). The difference is that here the intraluminal flow dynamics are not altered, and only the bladder dynamics differ.

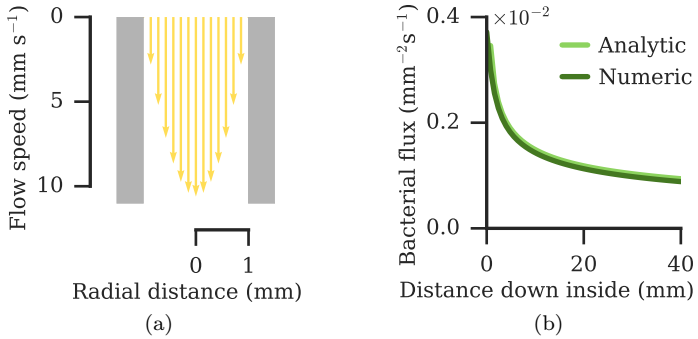

Figure 8: Solutions for the intraluminal flow profile and deposition onto the intraluminal surface. (a) The flow of urine through the catheter is parabolic (Poiseuille flow). (b) Bacterial flux onto the intraluminal surface. This is the number of bacteria sticking to the surface per unit time, for the density distribution shown in Fig. 2c of the main text. Dark green line: results of numerically simulating Eq. 3 and Eq. 10 of the main text. Light green line: the analytic result of Eq. 11 of the main text, for $x > 0.3$ mm.

Intraluminal flow

The hydrodynamics of flow through a pipe is well-established; the properties of the flow are determined by its Reynold's number [54]. We can calculate the Reynold's number for a "typical" catheter of lumen radius $R = 1$ mm, and urine flow rate of $\lambda = 1$ mL min^{-1}:

$$\mathrm{Re} = \frac{\lambda}{\pi R \nu} = \frac{\frac{1}{60}10^{-6}}{\pi 10^{-3} \cdot 0.83 \cdot 10^{-6}} \approx 6 \tag{B1}$$

where $\nu = 0.83$ mm^{2}s^{-1} is the kinematic viscosity of urine at 37 °C [55]. So for urine flowing through a catheter, the Reynold's number is low, ≈ 6, and the flow is Poiseuille (Fig. 8a).

In Eq. 3 of the main text, we assume that bacteria diffuse radially within the urine flow. We neglect both diffusion of bacteria in the longitudinal direction, and growth of bacteria within the flow. Examining the timescales of the problem justifies this. The timescale of bacterial growth is the doubling time, $\log 2/r_B = 1.8 \times 10^3$ s. The characteristic timescales for the radial and longitudinal diffusive processes are $R^2/D_B = 1 \times 10^4$ s and $L^2/D_B = 1.6 \times 10^7$ s. The typical timescale for the flow is the average time taken for urine to pass through the catheter, $\pi R^2 L/\lambda = 7.5$ s. The timescale of convective flow down the catheter is clearly much faster than the timescales of either of the diffusional processes, or growth. However we choose to include radial diffusion in the model because, although slow, it has significant effects over small radial distances, such as close to the catheter wall.

Connecting the different parts of the model

The different parts of the model are connected through coupling terms which preserve the total bacterial number. The various couplings are illustrated in Fig. 9, and described in detail in the following sections.

Connecting the extraluminal surface and bladder

The top of the catheter is within the bladder and immersed in urine. Therefore, bacteria may detach from the extraluminal surface of the catheter and join the planktonic population within the bladder. Conversely, bacteria within the urine in the bladder may stick to the extraluminal catheter surface, joining the biofilm there. Within the model, this coupling is incorporated into the extraluminal surface equation (Eq. 1 of the main text) as a flux at the top boundary. For the bladder, the coupling is a source term added to Eq. 2 of the main text. The coupling must conserve bacterial number, so the total number of bacteria moving to the bladder must equal the number leaving the catheter surface.

To derive the coupling terms (Eqs. 5 and 6 of the main text), we consider that only bacteria that are in the region of 'contact' between the extraluminal surface and bladder can migrate. Therefore, we need to define a contact surface (at the top of the catheter) and a contact volume (in the bladder surrounding the catheter) within which bacteria can transfer. Fig. 10 illustrates how we define these contact geometries. Assuming that a length l of catheter is exposed

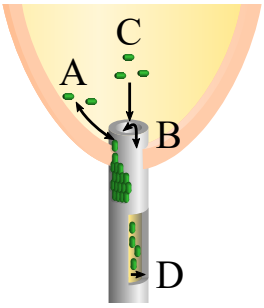

Figure 9: Connecting the different parts of the model. A: bacterial transfer between the top of the extraluminal surface and the bladder. B: Bacterial transfer between the top of the extraluminal surface and the top of the intraluminal surface. C: Bacterial transfer between the bladder and the intraluminal flow. D: Bacterial deposition from the intraluminal flow onto the intraluminal surface.

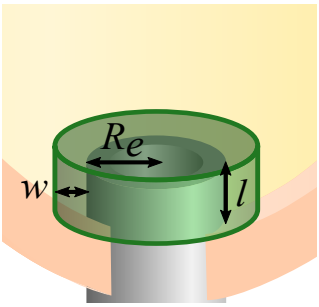

Figure 10: Illustrating the 'contact area' and 'contact volume'. Some bacteria within the bladder are close to the external catheter surface. At the top of the catheter, some bacteria on the surface are immersed in urine. If the catheter protrudes a distance l into the bladder, then there is a total surface contact area on the catheter of $S_c = 2\pi R_e l$. Suppose the bacteria within the bladder are 'in contact' with the catheter if they are within a distance w, and simplify this contact volume to be a cylinder of radius $R_e + w$ and height $l + w$. Then the contact volume is $V_c = \pi(R_e + w)^2(l + w) - \pi R_e^2 l$.

within the bladder, and that bacteria in the bladder within a distance w have a chance of sticking, we can write down the contact surface area and volume:

$$\begin{aligned} S_c &= 2\pi R_e l \\ V_c &= \pi(R_e + w)^2(l + w) - \pi R_e^2 l. \end{aligned} \tag{B2}$$

Here R_e is the external catheter radius, and l and w are as shown in Fig. 10.

Since we need to conserve the bacterial number, we must consider the absolute number of bacteria within the contact regions. $N_s = S_c \cdot n(L,t)$ is the number of bacteria on the catheter surface that are 'in contact' with the bladder, and $N_b = V_c \cdot \rho(t)$ is the the number of bacteria in the bladder that are 'in contact' with the catheter. Therefore, the flux of bacteria to the bladder is

$$\underbrace{k_d N_s}_{\text{detaching}} - \underbrace{k_a N_b}_{\text{attaching}} \tag{B3}$$

where k_d and k_a are respectively the rates at which bacteria detach from and attach to the catheter surface in the presence of urine; and N_s and N_b are the numbers of bacteria at the boundary on the outside of the catheter and in the bladder. To set reasonable values for k_d and k_a we make the following assumptions: any bacteria that are born on the exposed catheter surface detach, so $k_d = r_S$; and bacteria in the bladder are as sticky as possible and diffusing to the surface, so k_a is the Smoluchowski diffusion rate limited constant [31].

This makes it possible to write down the coupling terms. In the bladder there is a source term for the density,

$$\frac{k_d S_c n - k_a V_c \rho}{V}, \tag{B4}$$

where V is the total residual urine volume of the bladder. At the top of the catheter there is a corresponding surface

Parameter	Value
D_B	10^{-4} mm^{2}s^{-1}
λ	16.7 mm^{3}s^{-1}
R	1 mm
Re	6
L	40 mm

Table II: Typical parameter values for CAUTI

density flux at the boundary:

$$\frac{k_a V_c \rho - k_d S_c n}{S_c}. \tag{B5}$$

Eqs. B4 and B5 correspond to Eqs. 5 and 6 of the main text.

Connecting the intraluminal flow and intraluminal surface

Bacteria from the intraluminal flow are adsorbed onto the intraluminal surface. To calculate this numerically requires simulating the intraluminal flow, which is computationally expensive as it is a 2-dimensional problem, unlike the 1-dimensional surfaces elsewhere in the model.

Instead we model the adsorption of bacteria on the intraluminal surface using diffusion boundary theory, established by Levich [24]. In this theory, bacteria are modelled as particles which diffuse in the flow and adsorb on contact with the surface. The flow close to the surface becomes depleted of particles due to adsorption, hence particle deposition decreases with downstream distance (see Fig. 2c of the main text). The nature of this decrease depends on the geometry of the flow [24].

By making some assumptions, in particular neglecting surface forces (the so-called 'Smoluchowski-Levich' assumption) [56], and assuming the presence of a diffusion boundary layer [24], it is possible to write an analytic approximation for this bacterial flux to the catheter surface. To do this calculation of the bacterial flux we follow the path laid out by Levich in his book, Physiochemical hydrodynamics [24]. In particular, chapter 2.20, diffusion in laminar flow in a tube.

Summary

In the following we show how the maximal deposition of bacteria on the surface of a pipe can be approximated by

$$j(x) = D_B \left.\frac{\partial \sigma}{\partial y}\right|_{y=0} = 0.5835 D_B \rho \sqrt[3]{\frac{\lambda}{R^3 D_B}} \frac{1}{\sqrt[3]{x}}, \tag{B6}$$

which holds provided the Reynolds number Re < 2500 and $L \ll \lambda/D_B$. Here $j(x)$ is the bacterial flux to the surface, D_B is the bacterial bulk diffusivity, ρ is the initial bacterial density (at the entrance of the pipe), λ is the volume flow rate, R is the pipe radius, x is the longitudinal displacement, and L is the pipe length. Also, $\sigma(x, y)$ is the bacterial density within the fluid, and y is the perpendicular displacement from the surface (i.e. a planar approximation of the radial co-ordinate).

On a catheter we have typical values as given in Table II, so Eq. B6 can be seen to be valid. $L = 40$ and $\lambda/D_B \sim 10^5$, so $L \ll \lambda/D_B$, and Re $= 6$, so Re < 2500. Hence we can calculate the maximal deposition flux to be

$$j(x) \approx 0.003 \frac{\rho}{\sqrt[3]{x}}. \tag{B7}$$

Comparing the flux calculated from the numerical simulation with the analytic approximation shows good agreement, with more bacteria sticking at the top than further down (Fig. 8b).

Assumptions

1. All bacterial that contact the surface stick, i.e. the 'perfect sink' assumption. This is an absorbing boundary condition and leads to a maximal estimation for the deposition flux.

2. There are no external forces, except for the pressure differential driving the flow. This is the so-called 'Smoluchowski-Levich' assumption [56].

3. The flow within the pipe is laminar. This requires Re < 2500, and is valid beyond the initial hydrodynamic inlet region, $x > h \sim R \cdot \mathrm{Re}/27$. For our model catheter, Re ~ 6, and so $h \sim 0.2$ mm. Since the length of a catheter is 40–160 mm, the majority of the modelled catheter is in the laminar flow regime.

4. The diffusion profile is not fully established, and so there exists a thin diffusion boundary layer. The diffusion profile is fully established at a distance $H \sim \lambda/D_B$ down the pipe. Then for $x \ll H$, the boundary layer is extremely thin, and can be approximated as planar. So for the catheter, we require $L \ll \lambda/D_B$, which is the regime we are working in.

Solution

In the diffusion inlet region ($h < x \ll H$), diffusion occurs only close to the surface, and hence we can take a planar approximation, defining $y = R - r$ as a small variable. Then we want to solve the planar convection-diffusion equation,

$$v\frac{\partial \sigma}{\partial x} = D_B \frac{\partial^2 \sigma}{\partial y^2} \tag{B8}$$

where $v = \frac{2\lambda}{\pi R^2}\left(1 - \frac{r^2}{R^2}\right) = \frac{2\lambda}{\pi R^4}\left(2Ry - y^2\right)$. Since y is small, we expand v keeping only terms to first order in y, $v \approx \frac{4\lambda}{\pi R^3} y$. Then we can write

$$\frac{4\lambda}{\pi R^3} y \frac{\partial \sigma}{\partial x} = D_B \frac{\partial^2 \sigma}{\partial y^2}, \tag{B9}$$

with boundary conditions

$$\sigma = 0 \ \text{ at } y = 0, \qquad \sigma = \rho \ \text{ as } y \to \infty. \tag{B10}$$

We next introduce the dimensionless variable

$$\eta = \left(\frac{4\lambda}{\pi R^3 D_B}\right)^{\frac{1}{3}} \frac{y}{x^{1/3}}, \tag{B11}$$

to obtain

$$\frac{d^2\sigma}{d\eta^2} + \frac{1}{3}\eta^2 \frac{d\sigma}{d\eta} = 0, \tag{B12}$$

which can then be solved analytically. This gives an expression for σ,

$$\sigma(\eta) = \frac{\rho\sqrt[3]{3}}{\Gamma(\frac{1}{3})} \int_0^\eta \mathrm{e}^{-\frac{1}{9}z^3}\, dz, \tag{B13}$$

where Γ is the Gamma function. Finally we obtain the deposition flux

$$\begin{aligned} j(x) &= D_B \left(\frac{\partial \sigma}{\partial y}\right)_{y=0} \\ &= D_B \left(\frac{d\sigma}{d\eta}\frac{\partial \eta}{\partial y}\right)_{y=0} \\ &= \frac{D_B \rho}{\Gamma(\frac{1}{3})} \sqrt[3]{\frac{12\lambda}{\pi R^3 D_B}} \frac{1}{\sqrt[3]{x}} \\ &= 0.5835 D_B \rho \sqrt[3]{\frac{\lambda}{R^3 D_B}} \frac{1}{\sqrt[3]{x}}, \end{aligned} \tag{B14}$$

where the constant prefactor 0.5835 is obtained by numerical evaluation of $\frac{1}{\Gamma(1/3)}\sqrt[3]{12/\pi}$.

Appendix C: Nature of transitions

Criticality of urine production rate: washout transition

As discussed in the main text, there is a washout transition within the bladder model (Eq. 2 in main text). In this model for CAUTI, the bladder is modelled by logistic growth with dilution (Eq. 2):

$$\frac{d\rho}{dt} = r_B\rho\left(1 - \frac{\rho}{\kappa_B}\right) - k_D\rho$$

We can rearrange this slightly, in order to explore the effect of the dilution term.

$$\frac{d\rho}{dt} = (r_B - k_D)\rho\left(1 - \frac{r_B\rho}{(r_B - k_D)\kappa_B}\right) \tag{C1}$$

Written like this, we can see that this is a rescaled logistic growth equation:

$$\frac{d\rho}{dt} = r_{\text{eff}}\rho\left(1 - \frac{\rho}{\kappa_{\text{eff}}}\right), \tag{C2}$$

where we identify an effective growth rate, $r_{\text{eff}} = r_B - k_D$, and an effective carrying capacity $\kappa_{\text{eff}} = \frac{(r_B - k_D)\kappa_B}{r_B}$. From here we can observe that everything that is true for logistic growth must also be true here. We must have a steady state bacterial density equal to κ_{eff}, i.e. $\kappa_B(1 - \frac{k_D}{r_B})$. And hence as $k_D \to r_B$, $\kappa_{\text{eff}} \to 0$, and thus the steady state bacterial density goes to zero. Not only does the steady state density decrease with dilution rate, down to 0 at $k_D = r$, but the time taken to achieve steady state increases too. This is because $r_{\text{eff}} = r_B - k_D$. That is, the bacteria grow slower, and reach a lower population density as the dilution rate increases.

Bladder to surface regime transition

The timescale over which bacteriuria or blockages develop is the combination of the time taken for bacteria to ascend the catheter, and the time taken for bacteria to proliferate within the urine. Depending on the patient, catheter and bacterial characteristics, there can be three different regimes: a surface dominated regime, a bladder dominated regime, and a mixed regime. The relevant dimensionless number for these regimes is the ratio of the two timescales, ascension and proliferation. That is, the ratio of the characteristic time of the Fisher wave, and the characteristic time of growth within the bladder:

$$\alpha = \frac{L}{\sqrt{r_S D_S}} \Big/ \frac{\ln(\kappa_{\text{eff}}/\rho_0)}{r_{\text{eff}}} = \frac{(r_B - k_D)L}{\ln\left(\frac{\kappa_B}{\rho_0}(1 - \frac{k_D}{r_B})\right)\sqrt{r_S D_S}}. \tag{C3}$$

When $\alpha \gg 1$, we are in the surface dominated regime, and the urethral length and bacterial surface motility determine the infection timescale. While when $\alpha \ll 1$, we are in the bladder dominated regime, and the bacterial growth rate in the urine, and the urine production rate determine the infection timescale instead. The mixed regime occurs when $\alpha \approx 1$, and all of the above properties contribute to the infection timescale. For the model values given in the main text table 1, and $\rho_0 = 1$ (since growth in the bladder occurs as soon as a single bacterium is present), $\alpha \approx 100$, and the surface properties dominate the infection timescale, as observed. If, as discussed in the main text results (and in main text Fig. 5), the bacterial surface motility were as high as $D_S = 10^{-4}$ mm^{2}s^{-1}, we would instead have $\alpha \approx 1$, and be well within the mixed regime.

Appendix D: Numerical implementation of model

The model is implemented as three discrete equations (extraluminal surface, bladder, and intraluminal surface), coupled to one another and stepping forward in time. A forward-time centred-space (FTCS) method is used for both the extraluminal and intraluminal surface, with the bladder being solved with a forward Euler method.

Extraluminal surface

Recall Eq. 1 from the main text:

$$\frac{\partial n}{\partial t} = D_S \frac{\partial^2 n}{\partial x^2} + r_S n \left(1 - \frac{n}{\kappa_S}\right).$$

This can be discretised (with FTCS) as:

$$n_p^{i+1} = \frac{D_S \Delta t}{\Delta x^2}\left(n_{p+1}^i - 2n_p^i + n_{p-1}^i\right) + (1 + r_S \Delta t)\, n_p^i - \frac{r_S \Delta t}{\kappa_S}\left(n_p^i\right)^2, \tag{D1}$$

where n_p^i is the extraluminal bacterial surface density, $n(x,t)$, at the pth discrete position, and the ith time step; Δt is the time step; and Δx is the spatial discretisation. This has been shown to be numerically stable provided [57]:

$$\begin{aligned} \Delta x &< \sqrt{\frac{D_S}{r_S}} \\ \Delta t &< \frac{\Delta x^2}{2D_S} \end{aligned} \tag{D2}$$

which for the parameter values in Table 1 in the main text are 0.007 mm and 2000 s respectively. In this work, the values chosen for the step sizes were $\Delta x = \frac{1}{2}\sqrt{\frac{D_S}{r_S}}$, and $\Delta t = \frac{\Delta x^2}{20 D_S}$, which for the parameter values given in table 1 of the main text are $\Delta x = 0.003$ mm, and $\Delta t = 45$ s.

Since bacteria are free to diffuse between the extraluminal and intraluminal surfaces of the bladder, if there are $N = L/\Delta x$ discrete spatial positions, then $n_{N+1}^i = m_0^i$ (main text Eq. 7). The extraluminal surface is coupled with the bladder, with flux given by Eq. B5:

$$\frac{k_a V_c \rho - k_d S_c n}{S_c},$$

so at the top of the catheter, n_N is incremented as

$$n_N^{i+1} = \frac{D_S \Delta t}{\Delta x^2}\left(m_0^i - 2n_N^i + n_{N-1}^i\right) + (1 + r_S \Delta t)\, n_N^i - \frac{r_S \Delta t}{\kappa_S}\left(n_N^t\right)^2 + \frac{1}{2\pi R_e \Delta x}\left(k_a V_c \rho^i - k_d S_c n_N^i\right). \tag{D3}$$

Bladder

Including the coupling with the outside surface, Eq. 2 from the main text becomes:

$$\frac{d\rho}{dt} = r_B \rho \left(1 - \frac{\rho}{\kappa_B}\right) - k_D \rho + \frac{k_d S_c}{V} n(x{=}L) - \frac{k_a V_c}{V}\rho. \tag{D4}$$

Discretising this with a forward Euler method gives

$$\rho^{i+1} = \rho_i + \Delta t \left(\left(r_B - k_D - \frac{k_a V_c}{V}\right)\rho^i - \frac{r_B}{\kappa_B}\left(\rho^i\right)^2 + \frac{k_d S_c}{V} n_N^i \right), \tag{D5}$$

where ρ^i is the bladder bacterial volume density at the ith time step. The stability can be evaluated by comparison with the logistic map, as follows. Since we know that n_N^i is directly coupled to ρ^i, we can approximate Eq. D5, as

$$\begin{aligned} \rho^{i+1} &= \left(1 + \Delta t \left(r_B - k_D - \frac{k_a V_c}{V} + \frac{k_d S_c}{V}\right)\right)\rho^i + \frac{r_B \Delta t}{\kappa_B}\left(\rho^i\right)^2 \\ &= (1 + A\Delta t)\rho^i + \frac{r_B \Delta t}{\kappa_B}\left(\rho^i\right)^2 \end{aligned} \tag{D6}$$

which, with a change of variables $u^i = -\frac{r_B \Delta t}{\kappa_B (1 + A\Delta t)}\rho^i$, becomes

$$u^{i+1} = (1 + A\Delta t)\, u^i (1 - u^i), \tag{D7}$$

which stably converges to its non-zero equilibrium (see Murray chapter 2.3 [21]) for $1 < 1 + A\Delta t < 2$, i.e.

$$\Delta t < 1 \Big/ \left(r_B - k_D - \frac{k_a V_c}{V} + \frac{k_d S_c}{V}\right) \sim 10^4 \text{ s}. \tag{D8}$$

Intraluminal surface

Recall Eq. 4 from the main text:

$$\frac{\partial m}{\partial t} = D_S \frac{\partial^2 m}{\partial x^2} + r_S m \left(1 - \frac{m}{\kappa_S}\right) + j(x).$$

The bacterial flux, $j(x)$, comes from the deposition of bacteria onto the intraluminal surface from the urine flow out of the bladder. Here we take the analytic approximation for the bacterial flux, as given by Eq. B6 above (also main text Eq. 11),

$$j(x) = 0.5835 D_B \rho \sqrt[3]{\frac{\lambda}{R^3 D_B}} \frac{1}{\sqrt[3]{x}}.$$

This analytic solution is valid for $h < x \ll H$, i.e. the region in which the hydrodynamic flow is established, but the diffusive boundary layer is still small. The hydrodynamic establishment distance, h, is the distance at which the hydrodynamic boundary layer thickness is equal to the catheter radius. From Levich [24], defining the hydrodynamic boundary layer thickness as the thickness at which the flow speed is 90% of the main flow speed, this establishment distance occurs at

$$h \sim \frac{\mathrm{Re} \cdot R}{27} \sim 0.22 \text{ mm}. \tag{D9}$$

Behaviour within the early region, $x < h$, would be highly dependent on the exact geometry of the catheter, which is not incorporated into this model. Instead, knowing that the bacterial deposition must always be finite, we take a zeroth order approximation that the flux for $x < h$ is constant, and $j(x < h) = j(h)$. Since this is only a very small region of the catheter, this approximation has little impact on the results of the model.

Thus, we can discretise the intraluminal surface in a manner similar to the extraluminal surface; using a FTCS method gives

$$m_p^{i+1} = \frac{D_S \Delta t}{\Delta x^2}\left(m_{p+1}^i - 2m_p^i + m_{p-1}^i\right) + (1 + r_S \Delta t)\, m_p^i - \frac{r_S \Delta t}{\kappa}\left(m_p^i\right)^2 + 0.5835\left(\frac{\lambda D_B^2}{R^3}\right)^{1/3} \rho^i (p\Delta x)^{-1/3}, \tag{D10}$$

where m_p^i is the intraluminal bacterial surface density at the pth spatial point, and the ith time step. This is numerically stable under the same conditions as the extraluminal surface, provided the conditions discussed above hold for the validity of $j(x)$. That is, $L \ll 10^5$ mm. At the top of the catheter, bacteria can diffuse between the intraluminal surface and the extraluminal surface, so at the top of the catheter m_0 is incremented as

$$m_0^{i+1} = \frac{D_S \Delta t}{\Delta x^2}\left(m_1^i - 2m_0^i + n_N^i\right) + (1 + r_S \Delta t)\, m_0^i - \frac{r_S \Delta t}{\kappa}\left(m_0^i\right)^2 + 0.5835\left(\frac{\lambda D_B^2}{R^3}\right)^{1/3} \rho^i (\Delta x)^{-1/3}. \tag{D11}$$

Boundary and initial conditions

Within the results we explore four different boundary/initial conditions, corresponding to four different proposed infection origins.

1. If the infection originates from the skin, this is a Dirichlet boundary condition for the base of the extraluminal surface, $n_0^i = const.$, and a Neumann (reflecting) boundary condition for the base of the intraluminal surface, $m_{N+1}^i = m_{N-1}^i$.
2. If the infection originates from the drainage bag, this is a Dirichlet boundary condition for the base of the intraluminal surface, $m_N^i = const.$, and a Neumann (reflecting) boundary condition for the base of the extraluminal surface, $n_1^i = n_{-1}^i$.
3. If there is uniform initial contamination across the extraluminal surface, this is an initial condition $n_p^0 = const.$, with reflecting boundary conditions for both the intraluminal and extraluminal surfaces, $m_{N+1}^i = m_{N-1}^i$ and $n_1^i = n_{-1}^i$.
4. Finally, if the bladder is already contaminated before the catheter is inserted, this is an initial condition for the bladder, ρ_0, and again there are reflecting boundary conditions for the catheter surfaces.

[1] Suman Prinjha and Alison Chapple. Living with an indwelling urinary catheter. *Nursing Times*, 109(44):12–14, 2013.
[2] Vrad Levering, Qiming Wang, Phanindhar Shivapooja, Xuanhe Zhao, and Gabriel P. López. Soft robotic concepts in catheter design: An on-demand fouling-release urinary catheter. *Advanced Healthcare Materials*, 3(10):1588–1596, 2014.
[3] Lindsay E. Nicolle. Catheter associated urinary tract infections. *Antimicrobial Resistance and Infection Control*, 3(23), 2014.
[4] Thomas M. Hooton, Suzanne F. Bradley, Diana D. Cardenas, Richard Colgan, Suzanne E. Geerlings, James C. Rice, Sanjay Saint, Anthony J. Schaeffer, Paul A. Tambayh, Peter Tenke, and Lindsay E. Nicolle. Diagnosis, Prevention, and Treatment of Catheter-Associated Urinary Tract Infection in Adults: 2009 International Clinical Practice Guidelines from the Infectious Diseases Society of America. *Clinical Infectious Diseases*, 50(5):625–663, 2010.
[5] Shelley S. Magill, Jonathan R. Edwards, Wendy Bamberg, Zintars G. Beldavs, Ghinwa Dumvati, Marion A. Kainer, Ruth Lynfield, Meghan Maloney, Laura McAllister-Hollod, Joelle Nadle, Susan M. Ray, Deborah L. Thompson, Lucy E. Wilson, and Scott K. Fridkin. Multistate Point-Prevalence Survey of Health Care–Associated Infections. *New England Journal of Medicine*, 370(13):1198–1208, 2014.
[6] Eyal Zimlichman, Daniel Henderson, Orly Tamir, Calvin Franz, Peter Song, Cyrus K. Yamin, Carol Keohane, Charles R. Denham, and David W. Bates. Health care-associated infections: A Meta-analysis of costs and financial impact on the US health care system. *JAMA Internal Medicine*, 173(22):2039–2046, 2013.
[7] Dawn M. Sievert, Philip Ricks, Jonathan R. Edwards, Amy Schneider, Jean Patel, Arjun Srinivasan, Alex Kallen, Brandi Limbago, and Scott K. Fridkin. Antimicrobial-Resistant Pathogens Associated with Healthcare-Associated Infections Summary of Data Reported to the National Healthcare Safety Network at the Centers for Disease Control and Prevention, 2009–2010. *Infection Control & Hospital Epidemiology*, 34(1):1–14, 2013.
[8] Craig A. Umscheid, Matthew D. Mitchell, Jalpa A. Doshi, Rajender K. Agarwal, Kendal Williams, and Patrick J. Brennan. Estimating the Proportion of Healthcare-Associated Infections That Are Reasonably Preventable and the Related Mortality and Costs. *Infection Control & Hospital Epidemiology*, 32(2):101–114, 2011.
[9] Roger C. L. Feneley, Ian B. Hopley, and Peter N. T. Wells. Urinary catheters: history, current status, adverse events and research agenda. *Journal of Medical Engineering & Technology*, 39(8):459–470, 2015.
[10] Evelyn Lo, Lindsay E. Nicolle, Susan E. Coffin, Carolyn V. Gould, Lisa L. Maragakis, Jennifer A. Meddings, David A. Pegues, Ann Marie Pettis, Sanjay Saint, and Deborah S. Yokoe. Strategies to Prevent Catheter-Associated Urinary Tract Infections in Acute Care Hospitals: 2014 Update. *Infection Control & Hospital Epidemiology*, 35(05):464–479, 2014.
[11] Carolyn V. Gould, Craig A. Umscheid, Rajender K. Agarwal, Gretchen Kuntz, and David A. Pegues. Guidelines for prevention of catheter-associated urinary tract infections. *Infection Control and Hospital Epidemiology*, 31(4):319–326, 2010.
[12] Jennifer A. Meddings, Mary A. M. Rogers, Sarah L. Krein, Mohamad G. Fakih, Russell N. Olmsted, and Sanjay Saint. Reducing unnecessary urinary catheter use and other strategies to prevent catheter-associated urinary tract infection: an integrative review. *BMJ Qual Saf*, 23:277–289, 2014.
[13] Sanjay Saint and Benjamin A Lipsky. Preventing catheter-related bacteriuria should we? can we? how? *Arch Intern Med*, 158:800–808, 1999.
[14] Helen Godfrey. Living with a long-term urinary catheter: Older people's experiences. *Journal of Advanced Nursing*, 62(2):180–190, 2008.
[15] Allison S. Letica-Kriegel, Hojjat Salmasian, David K. Vawdrey, Brett E. Youngerman, Robert A. Green, E. Yoko Furuya, David P. Calfee, and Rimma Perotte. Identifying the risk factors for catheter-associated urinary tract infections: A large cross-sectional study of six hospitals. *BMJ Open*, 9, 2 2019.
[16] Rodney M. Donlan. Biofilms and device-associated infections. *Emerging Infectious Diseases*, 7(2):277–281, 2001.
[17] Nicolas W. Cortes-Penfield, Barbara W. Trautner, and Robin L.P. Jump. Urinary tract infection and asymptomatic bacteriuria in older adults. *Infectious Disease Clinics of North America*, 31:673–688, 12 2017.
[18] David M. Gordon and Margaret A. Riley. A theoretical and experimental analysis of bacterial growth in the bladder. *Molecular Microbiology*, 6(4):555–562, 1992.
[19] Roger C. L. Feneley, Calvin M. Kunin, and David J. Stickler. An indwelling urinary catheter for the 21st century. *BJU International*, 109:1746–1749, 2011.
[20] Maurice M. Garcia, Shelly Gulati, Dorian Liepmann, G. Bennett Stackhouse, Kirsten Greene, and Marshall L. Stoller. Traditional Foley Drainage Systems-Do They Drain the Bladder? *Journal of Urology*, 177(1):203–207, 2007.
[21] James D. Murray. *Mathematical Biology: I: An Introduction.* Springer-Verlag, New York, 3rd edition, 2002.
[22] Geoffrey I. Taylor. Dispersion of soluble matter in solvent flowing slowly through a tube. *Proceedings of the Royal Society of London. Series A. Mathematical and Physical Sciences*, 219(1137):186–203, 1953.
[23] M. J. Lighthill. Initial development of diffusion in poiseuille flow. *IMA Journal of Applied Mathematics (Institute of Mathematics and Its Applications)*, 2(1):97–108, 1966.
[24] Veniamin G. Levich. *Physicochemical hydrodynamics.* Prentice-Hall, Englewood Cliffs, N.J., 1962.
[25] Anatolij Gelimson, Kun Zhao, Calvin K. Lee, W. Till Kranz, Gerard C. L. Wong, and Ramin Golestanian. Multicellular Self-Organization of P. aeruginosa due to Interactions with Secreted Trails. *Physical Review Letters*, 117(17), 2016.
[26] Jonathan Saragosti, Pascal Silberzan, and Axel Buguin. Modeling E. coli Tumbles by Rotational Diffusion. Implications for Chemotaxis. *PloS one*, 7(4), 2012.
[27] Hans Bremer and Patrick P. Dennis. Modulation of Chemical Composition and Other Parameters of the Cell at Different

Exponential Growth Rates. *EcoSal Plus*, 3(1), 2008.
[28] Valerie S. Forsyth, Chelsie E. Armbruster, Sara N. Smith, Ali Pirani, A. Cody Springman, Matthew S. Walters, Greta R. Nielubowicz, Stephanie D. Himpsl, Evan S. Snitkin, and Harry L. T. Mobley. Rapid growth of uropathogenic Escherichia coli during human urinary tract infection. *mBio*, 9(2):1–13, 2018.
[29] David J. Stickler. Bacterial biofilms in patients with indwelling urinary catheters. *Nature Clinical Practice Urology*, 5(11):598–608, 2008.
[30] Guennadi Sezonov, Danièle Joseleau-Petit, and Richard D'Ari. Escherichia coli physiology in Luria-Bertani broth. *Journal of Bacteriology*, 189(23):8746–8749, 2007.
[31] M. Von Smoluchowski. Versucheiner Mathematischen Theorie der Koagulations Kinetic Kolloider Lousungen. *Z. Phys. Chem.*, 92:129–168, 1917.
[32] Rosalind J. Allen and Bartłomiej Waclaw. Bacterial growth: A statistical physicist's guide. *Reports on Progress in Physics*, 82(1), 2019.
[33] S. John Pirt. *Principles of Microbe and Cell Cultivation.* Blackwell Scientific Publications, Oxford, 1975.
[34] Thomas Bjarnsholt. The Role of Bacterial Biofilms in Chronic Infections. *APMIS*, 121(SI):1–58, 2013.
[35] John W. Warren. CATHETER-ASSOCIATED URINARY TRACT INFECTIONS. *International Journal of Antimicrobial Agents*, 17:299–303, 2001.
[36] S. M. Jacobsen, David J. Stickler, Harry L. T. Mobley, and M. E. Shirtliff. Complicated Catheter-Associated Urinary Tract Infections Due to Escherichia coli and Proteus mirabilis. *Clinical Microbiology Reviews*, 21(1):26–59, 2008.
[37] Sandra A. Wilks, Mandy J. Fader, and C. William Keevil. Novel insights into the proteus mirabilis crystalline biofilm using real-time imaging. *PLoS ONE*, 10(10):1–13, 2015.
[38] S. Mathur, N. A. Sabbuba, M. T. E. Sulle, D. J. Stickler, and R. C. L. Feneley. Genotyping of urinary and fecal *proteus mirabilis* isolates from individuals with long-term urinary catheters. *Eur. J. Clin. Microbiol. Infect. Dis.*, 24:643–644, 2005.
[39] Richard Daifuku and Walter E. Stamm. Association of Rectal and Urethral Colonization With Urinary Tract Infection in Patients With Indwelling Catheters. *JAMA: The Journal of the American Medical Association*, 252(15):2028–2030, 1984.
[40] Greta R. Nielubowicz and Harry L. T. Mobley. Host-pathogen interactions in urinary tract infection. *Nature Reviews Urology*, 7:430–441, 2010.
[41] Walter E. Stamm. Catheter-associated urinary tract infections: Epidemiology, pathogenesis, and prevention. *The American Journal of Medicine*, 91(3B):S65–S71, 1991.
[42] Thomas M. Hooton, Mariacristina Vecchio, Alison Iroz, Ivan Tack, Quentin Dornic, Isabelle Seksek, and Yair Lotan. Effect of increased daily water intake in premenopausal women with recurrent urinary tract infections: A randomized clinical trial. *JAMA Internal Medicine*, 178:1509–1515, 11 2018.
[43] Yair Lotan, Michel Daudon, Franck Bruyère, Glenn Talaska, Giovanni Strippoli, Richard J. Johnson, and Ivan Tack. Impact of fluid intake in the prevention of urinary system diseases: A brief review. *Current Opinion in Nephrology and Hypertension*, 22, 5 2013.
[44] Anna Mae Scott, Justin Clark, Chris Del Mar, and Paul Glasziou. Increased fluid intake to prevent urinary tract infections: Systematic review and meta-analysis. *British Journal of General Practice*, 70:E200–E207, 2020.
[45] Robert J. Broomfield, Sheridan D. Morgan, Azhar Khan, and David J. Stickler. Crystalline bacterial biofilm formation on urinary catheters by urease-producing urinary tract pathogens: A simple method of control. *Journal of Medical Microbiology*, 58(10):1367–1375, 2009.
[46] Roger D. Klein and Scott J. Hultgren. Urinary tract infections: microbial pathogenesis, host–pathogen interactions and new treatment strategies. *Nature Reviews Microbiology*, 18(4):211–226, 2020.
[47] Betsy Foxman. Urinary tract infection syndromes. Occurrence, recurrence, bacteriology, risk factors, and disease burden. *Infectious Disease Clinics of North America*, 28(1):1–13, 2014.
[48] I. Raad, W. Costerton, U. Sabharwal, M. Sacilowski, W. Anaissie, and G. Bodey. Ultrastructural analysis of indwelling vascular catheters: a quantitative relationship between luminal colonization and duration of placement. *J. Infect. Dis.*, 168:400–407, 1993.
[49] Heather Gage, Miriam Avery, Caragh Flannery, Peter Williams, and Mandy Fader. Community prevalence of long-term urinary catheters use in england. *Neurourology and Urodynamics*, 36:293–296, 2 2017.
[50] Calvin M. Kunin. Can we build a better urinary catheter? *New England Journal of Medicine*, 319(6):365–366, 1988.
[51] Richard Platt, B Frank Polk, Bridget Murdock, and Bernard Rosner. Risk factors for nosocomial urinary tract infection. *American Journal of Epidemiology*, 124:977–985, 1986.
[52] L. R. Band, L. J. Cummings, S. L. Waters, and J. A.D. Wattis. Modelling crystal aggregation and deposition in the catheterised lower urinary tract. *Journal of Mathematical Biology*, 59(6):809–840, aug 2009.
[53] Ana L. Flores-Mireles, Jennifer N. Walker, Michael G. Caparon, and Scott J. Hultgren. Urinary tract infections: Epidemiology, mechanisms of infection and treatment options. *Nature Reviews Microbiology*, 13(5):269–284, 2015.
[54] Steven Vogel. *Life in Moving Fluids.* Princeton University Press, Princeton, 2nd edition, 1994.
[55] Brant A. Inman, Wiguins Etienne, Rainier Rubin, Richmond A. Owusu, Tiago R. Oliveira, Dario B. Rodriques, Paolo F. Maccarini, Paul R. Stauffer, Alireza Mashal, and Mark W. Dewhirst. The impact of temperature and urinary constituents on urine viscosity and its relevance to bladder hyperthermia treatment. *International Journal of Hyperthermia*, 29(3):206–210, 2013.
[56] Henk J. Busscher and Henny C. Van Der Mei. Microbial adhesion in flow displacement systems. *Clinical Microbiology Reviews*, 19(1):127–141, 2006.
[57] K. M. Agbavon, A. R. Appadu, and M. Khumalo. On the numerical solution of Fisher's equation with coefficient of diffusion term much smaller than coefficient of reaction term. *Advances in Difference Equations*, 2019(146), 2019.